A Self-powered Autonomous Device for WIreless struCtural Health monitoring - the SANDWICH project

C A Featherston, K M Holford, R Pullin, J Lees, M Pearson, B J Greaves, O Wood, M Arnold, A Kural, K Thangaraj

Cardiff University, UK

Partners: MicroSemi, NEDEAS, Airbus

Technology Strategy Board
Driving Innovation

Content

- Motivation
- Background
  - Structural Health Monitoring
  - Energy Sources
- Vibration Energy Harvesting
  - Passive
  - Active
- Thermoelectric Energy Harvesting
- RF Energy Harvesting
- Power Management
- System Integration
- Conclusions

Motivation

- To reduce the environmental impact/cost of air travel aircraft need to be lighter
- This necessitates optimum use of material
- Smaller safety factors requires confidence in the structural integrity
- Must be achieved without lengthy downtime for routine inspection
- Solution lies in structural health monitoring (SHM)
- Energy harvesting provides the potential for a self powered wireless SHM system

Typical SHM System

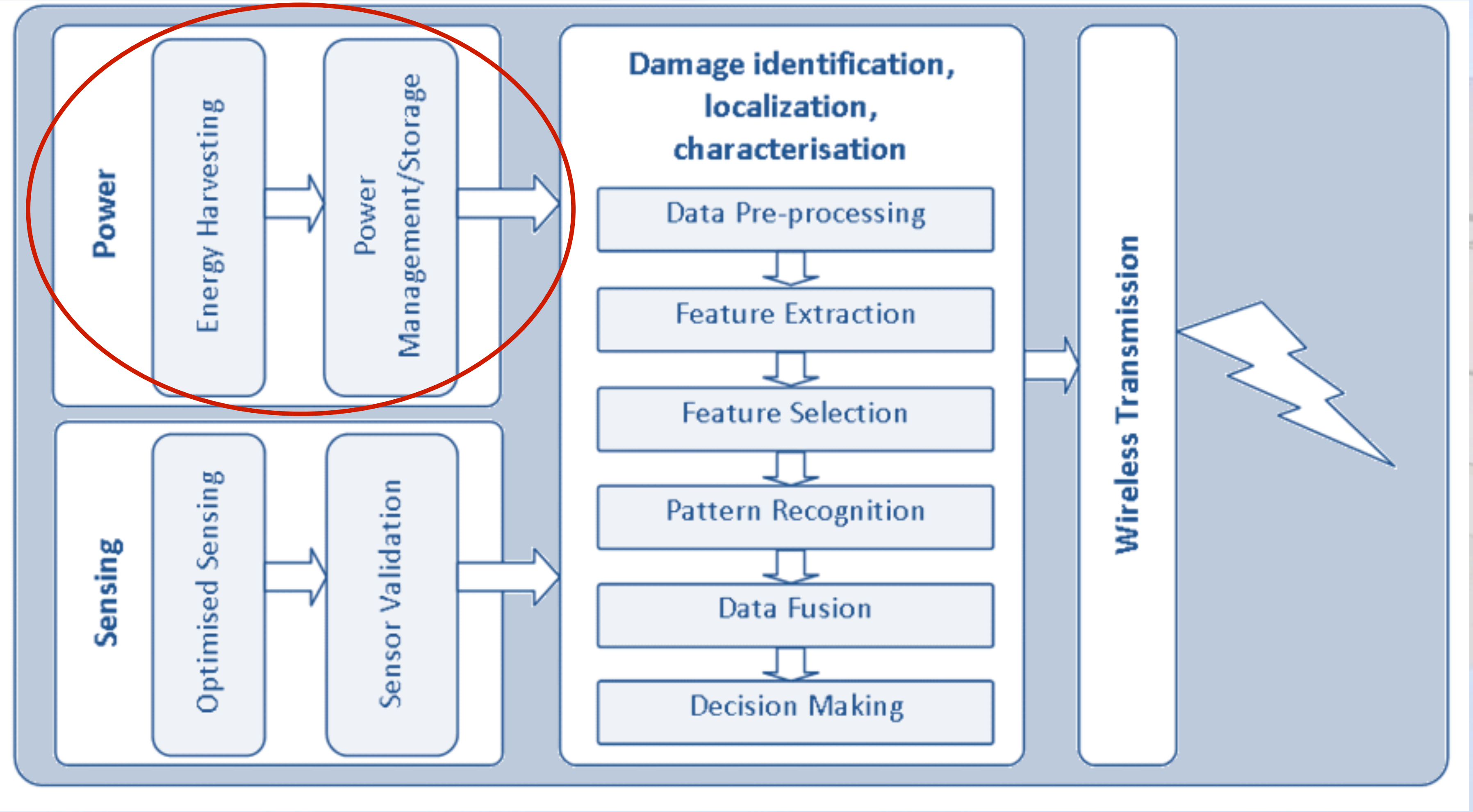

Power Requirements for Wireless Nodes

- Mistras 4 channel acoustic emission wireless board
- Power requirements typically in mW range dependant on application
- Input voltage 5V
- Power consumption
  - 10 mW sleep with timer wake up
  - 50 mW sleep with parametric wakeup
  - 170 mW full power

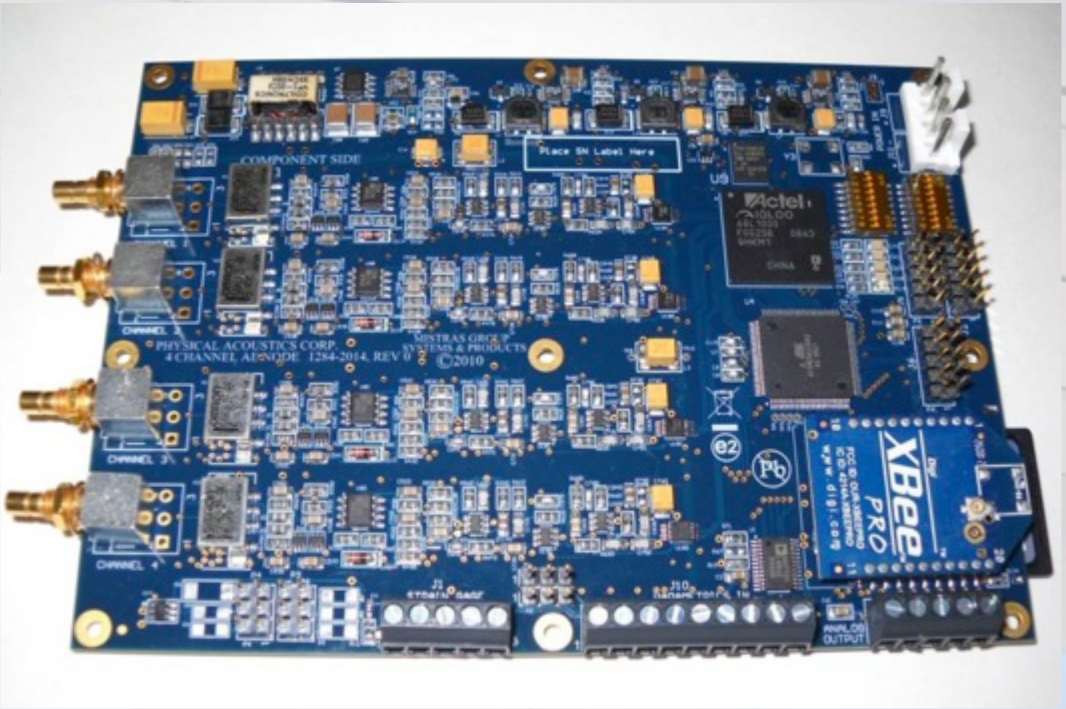

Energy Harvesting Sources

Energy Source	Power density	Reference
Acoustic Noise	0.003μW/cm³ @ 75Db 0.96 μW/cm³ @ 100Db	Rabaey, Ammer, Da Silva Jr, Patel and Roundy (2000)
Temperature Variation	10 μW/cm³	Roundy, Steingart, Frechette, Wright and Rabaey (2004)
Ambient Radio Frequency	1 μW/cm²	Yeatman (2004)
Ambient Light	100 mW/cm² (direct sun) 100 W/cm² (office lighting)	Available
Thermoelectric	60 W/cm²	Stevens (1999)
Vibration (micro generator)	4 W/cm3 (human motion Hz) 800 W/cm³ (machines kHz)	Mitcheson, Green, Yeatman and Holmes (2004)
Vibration (piezoelectric)	200 μW/cm³	Roundy, Wright and Pister (2002)
Airflow	1 μW/cm²	Holmes (2004)
Push buttons	50 J/N	Paradiso and Feldmeier (2001)
Shoe inserts	330 μW/cm²	Shenck and Paradiso (2001)
Hand generators	30 W/kg	Starner and Paradiso (2004)
Heel strike	7 W/cm²	Yaglioglu (2002) Shenck and Paradiso (2001)

Thermoelectric Energy Harvesting

Defining a reference temperature scenario

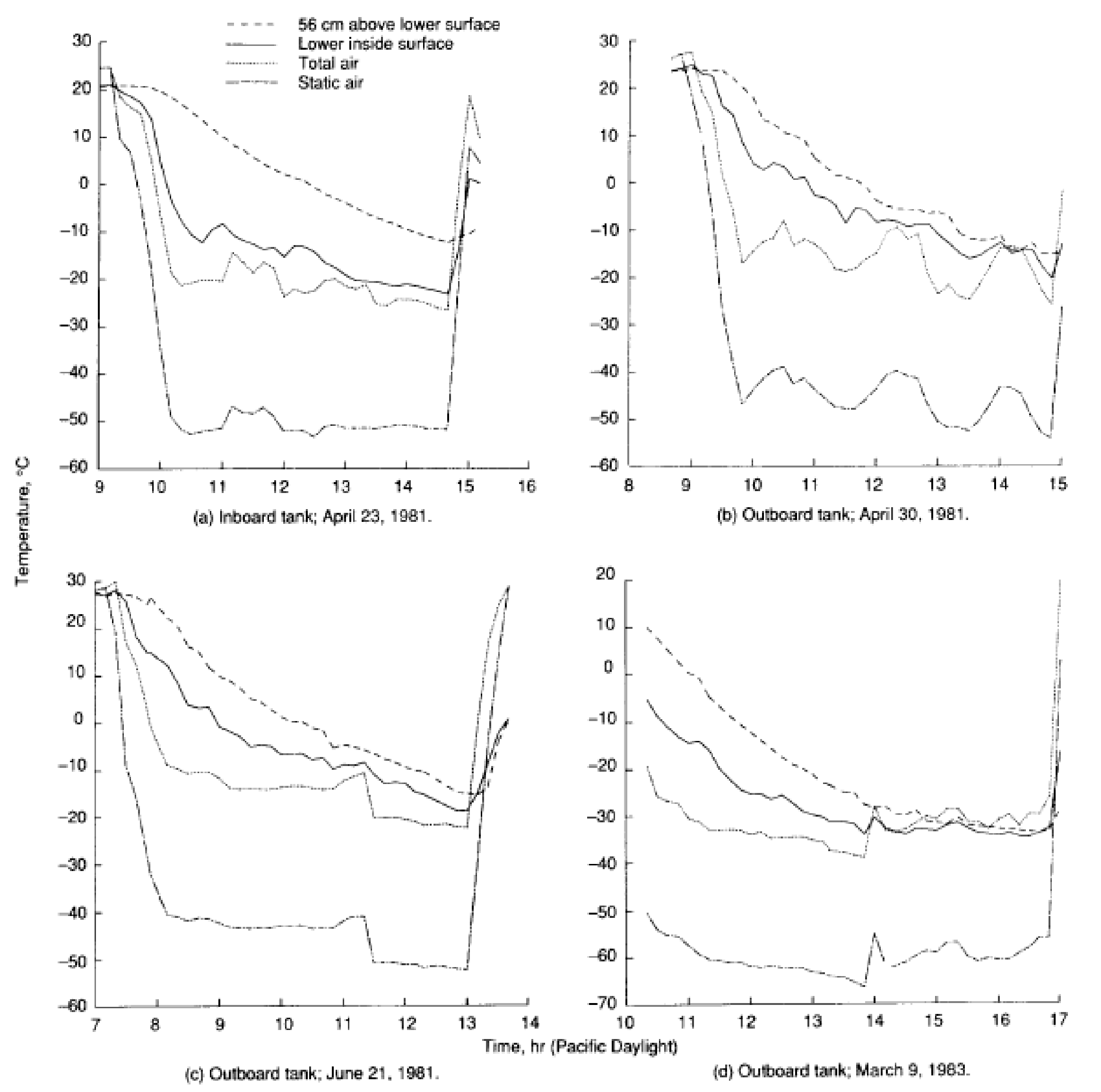

- Range of temp gradients developed
- Fuel/surroundings identified as providing most potential
- Thermocouples inside fuel tanks of Lockheed L1011
- Temperature differences of up to 30°C over significant time periods
- For temp diff 0-50°C at average temp -50-50°C most suitable material is bismuth telluride

•Svehla, R., 1990, *In-Flight and Simulated Aircraft Fuel Temperature Measurements*, http://ntrs.nasa.gov:80/archive/nasa/casi.ntrs.nasa.gov/19910006105_1991006105.pdf

Thermal model of power output based on real flight data

Initial model (Min and Rowe)

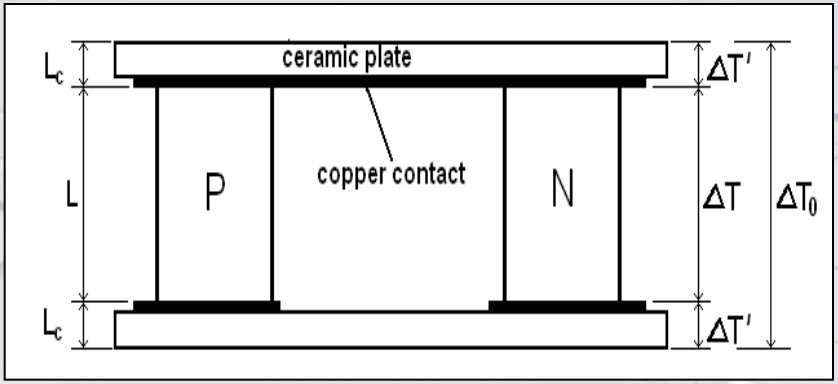

Incorporating boundary conditions

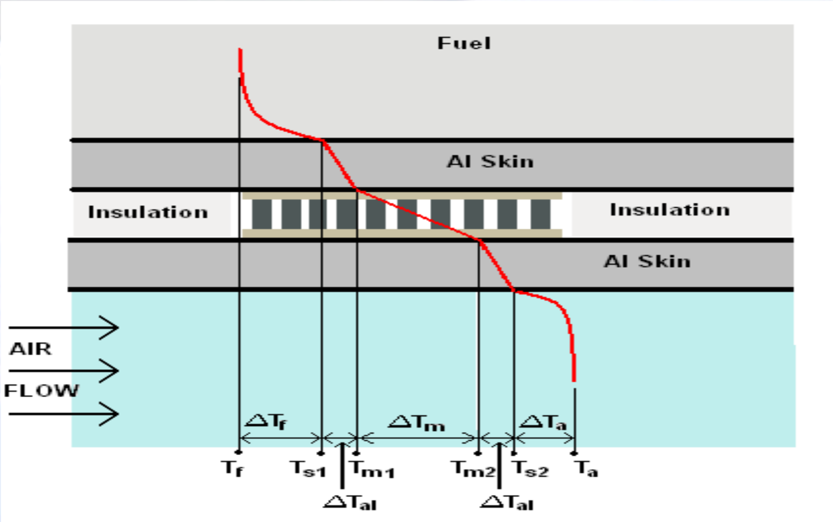

Temperature Difference/ Power Output –

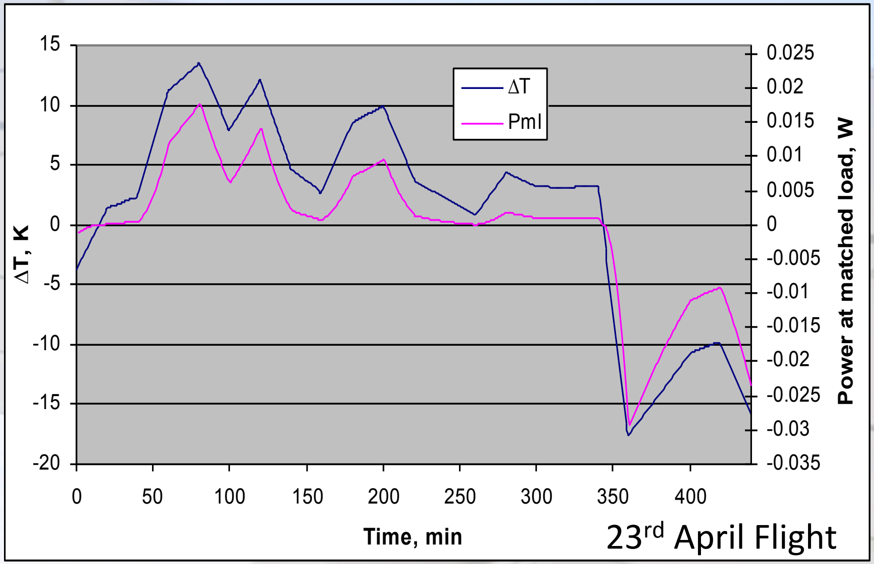

Energy Harvesting Potential

Flight	Inflow Energy, [J]	Outflow Energy, [J]	Total Energy, [J]	Average Power, [mW]
23 April 1981	88.26	86.90	175.16	6.65
30 April 1981	126.41	242.49	368.90	15.3
19 March 1983	248.28	339.16	587.43	22.3
21 Jun 1981	125.31	163.02	288.06	12.0
Average	147.07	207.20	354.89	14.06

Test Rig

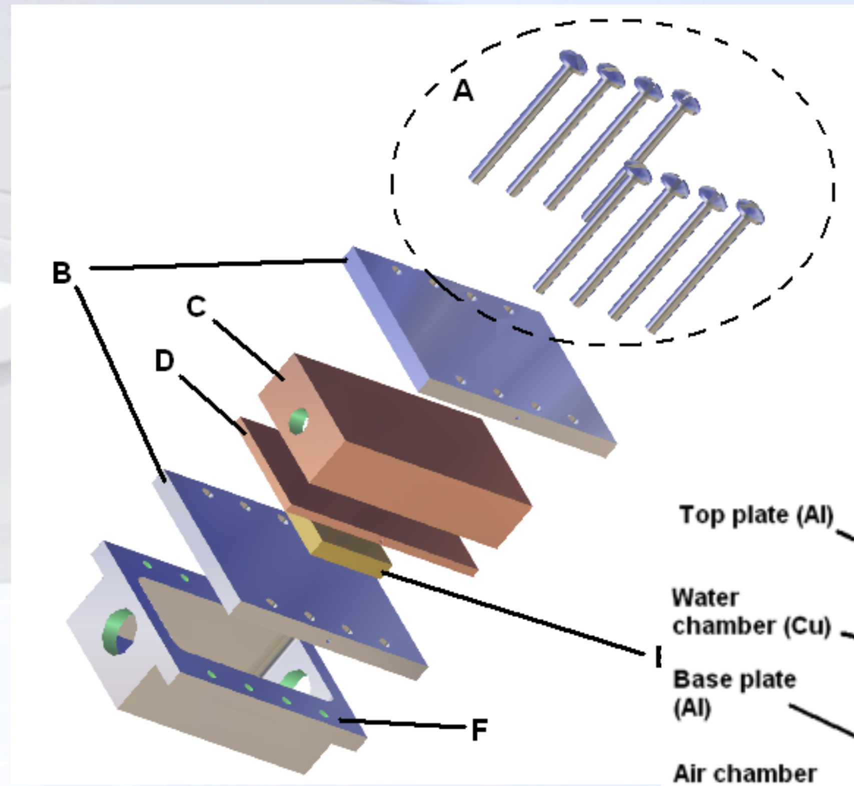
A
B
C
D
F

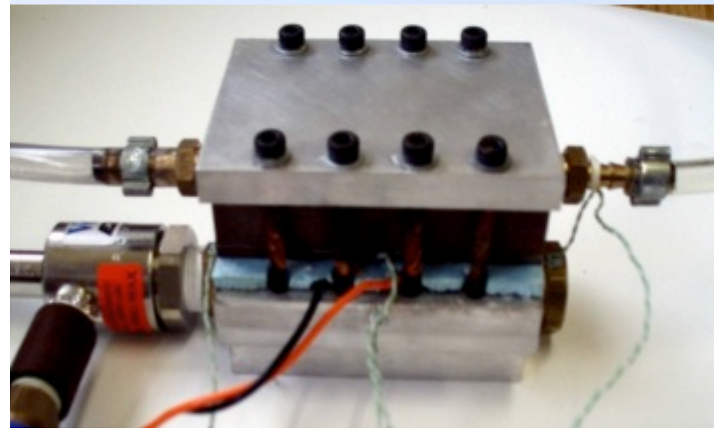

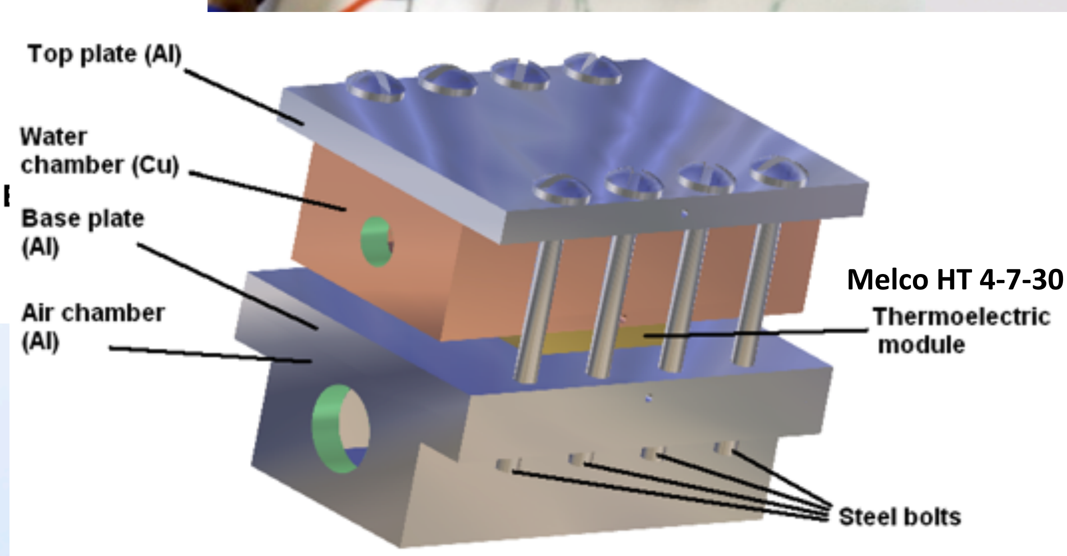
Top plate (Al)
Water chamber (Cu)
Base plate (Al)
Air chamber (Al)
Melco HT 4-7-30
Thermoelectric module
Steel bolts

Simulation

- Cargo Bay
  - Skin - Primary insulation
- Hydraulics
  - 2 hydraulic Pipelines
- Waste Water
  - Waste water tank, Ambient
- Crown Area
  - Skin, Primary insulation, Ambient)
- E-bay
  - Fuselage, Primary Insulation, Ambient
- Cabin
  - Fuselage, Primary Insulation, Secondary Insulation

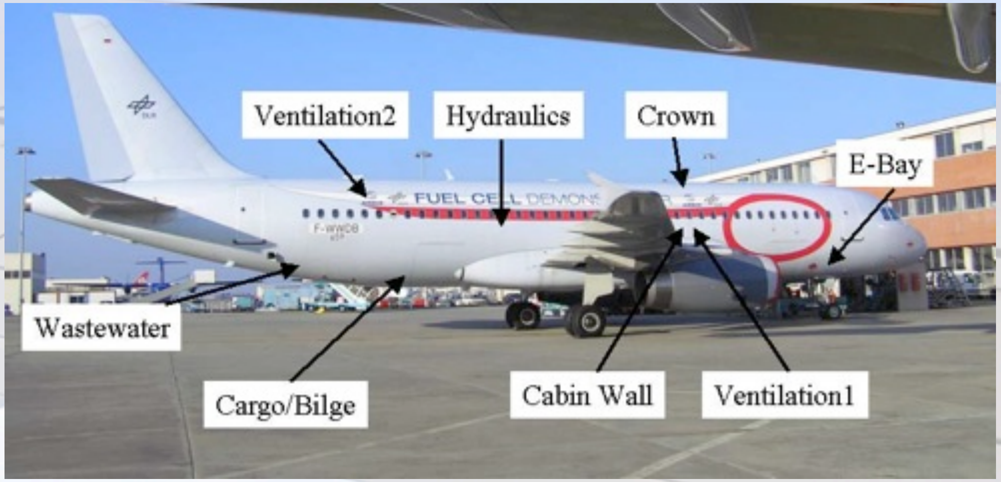

Results

Temperature Differential Between:	Peak Temperature Differential, K	Peak Power, mW	Average Power, mW
Hydraulic Skin 1 Ambient	19.50	6.43	3.09
Hydraulic Skin 1 Hydraulic Skin 2	22.70	8.60	3.46
Waste Water Skin Waste Water Ambient	18.80	6.10	3.41
Crown Fuselage Crown Primary Insulation	42.90	29.70	10.13
Crown Fuselage Crown Ambient	42.00	28.50	10.20
E-Bay Fuselage E-Bay Primary Insulation	34.80	19.78	5.84
E-Bay Fuselage E-Bay Ambient	40.60	26.68	8.12
Cabin Fuselage Cabin Primary Insulation	29.40	14.27	3.58
Cabin Fuselage Cabin Secondary Insulation	44.10	31.34	10.89
Cabin Primary Insulation Cabin Secondary Insulation	20.30	6.99	2.27

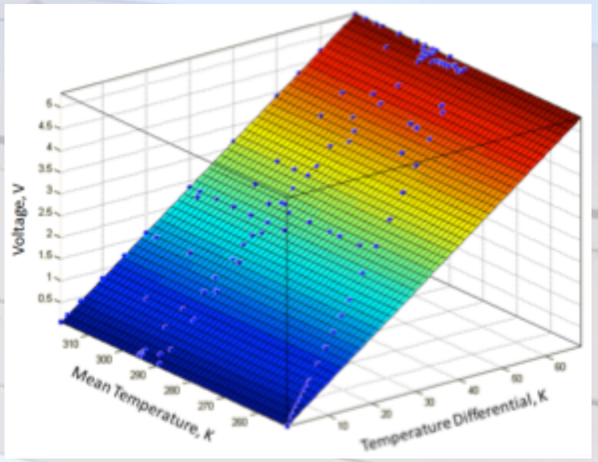

- Simulated power output for Micropelt MPG-D751
- Utilised "mypelt" simulation tool
- Indicated possibility of generating average power levels of 3-10mW

CARDIFF UNIVERSITY
PRIFYSGOL CAERDYDD

Vibration Energy Harvesting

Vibration generated in an aircraft wing panel

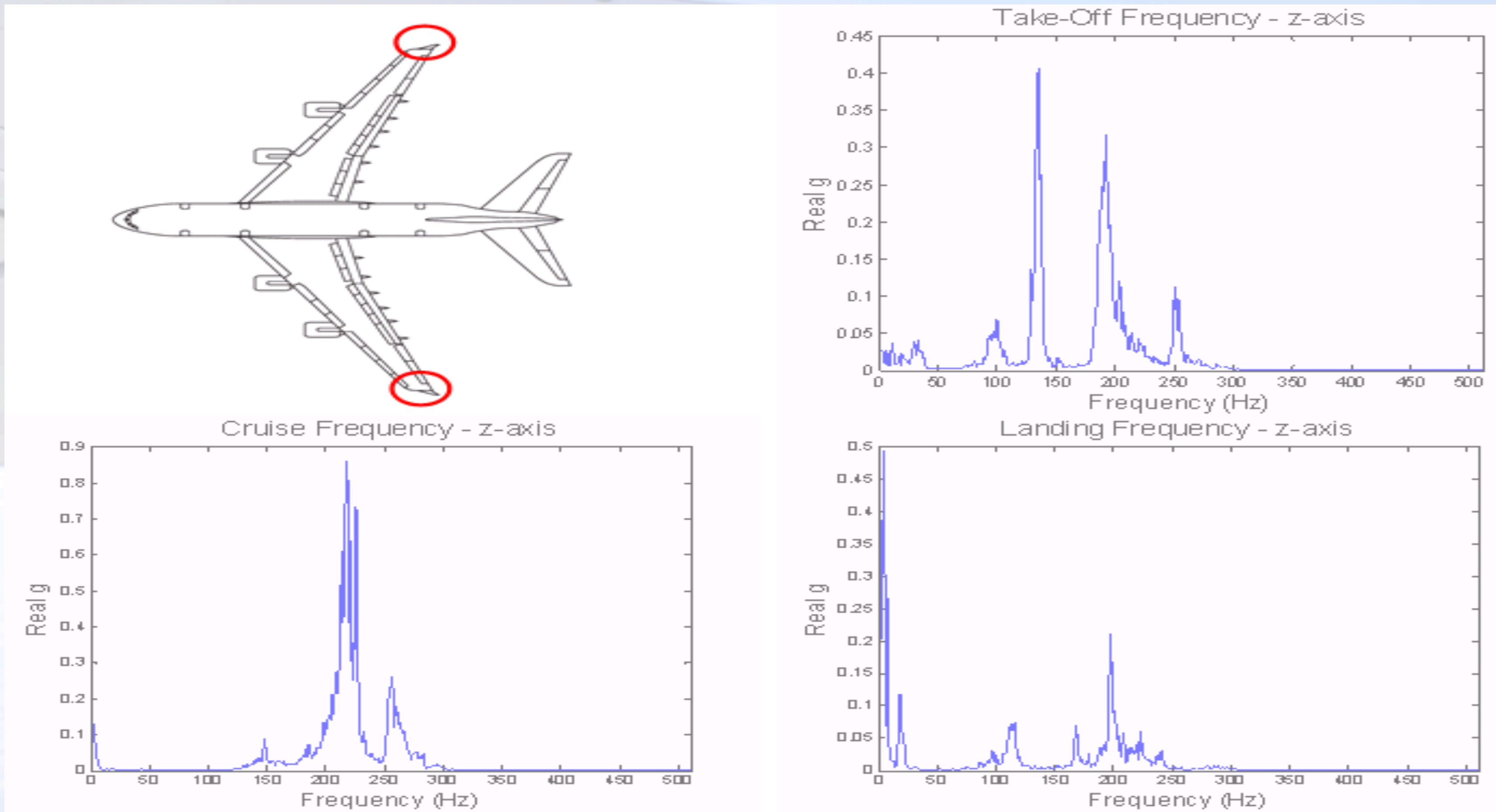

Frequencies between 0 – 300Hz, accelerations up to 0.9g

Piezoelectric Energy Harvesters

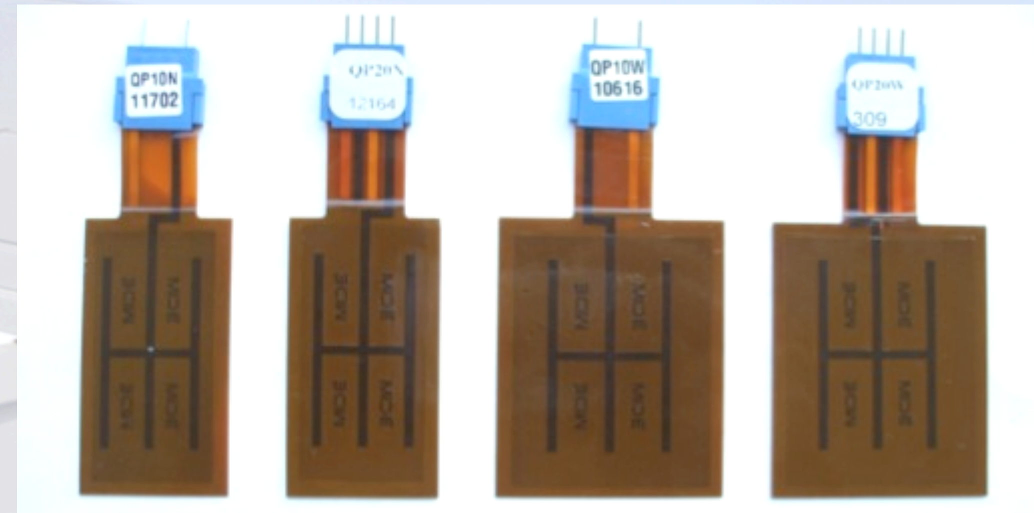

Mide QP10n, QP10w, QP20n and QP20w piezoelectric transducers

Product	QP10n	QP10w	QP20n	QP20w
Piezo Layers	1 x 10-mil [US]	1 x 10-mil [US]	2 x 10-mil [US]	2 x 10-mil [US]
Device Size [in]	2.00 x 1.00 x 0.015	2.00 x 1.50 x 0.015	2.00 x 1.00 x 0.03	2.00 x 1.50 x 0.03
Active Size [inches]	1.81 x 0.81 x 0.01	1.81 x 1.31 x 0.01	2 x (1.81 x 0.81 x 0.01)	2 x (1.81 x 1.31 x 0.01)
Weight [oz]	0.1	0.1	0.17	0.28
Capacitance [μF]	0.06	0.06	0.12	0.20
Voltage Range [V]	± 200	± 200	± 200	± 200
Full-scale Strain [με]	± 262	± 278	± 264	± 280

Design of a Potential Demonstrator

Test panel

Frame

Electromagnetic shaker

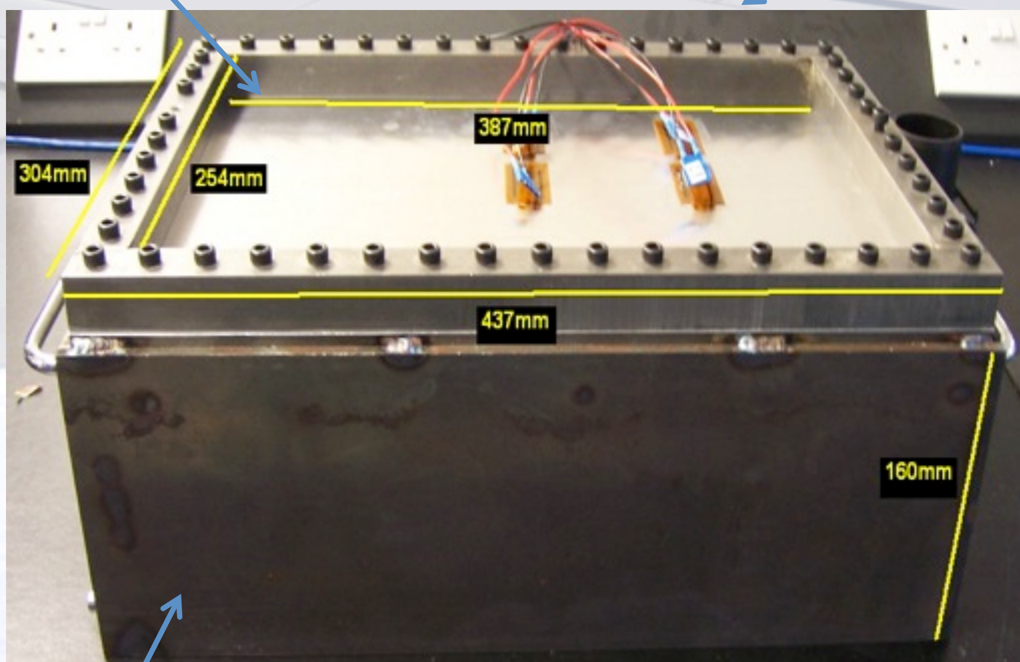

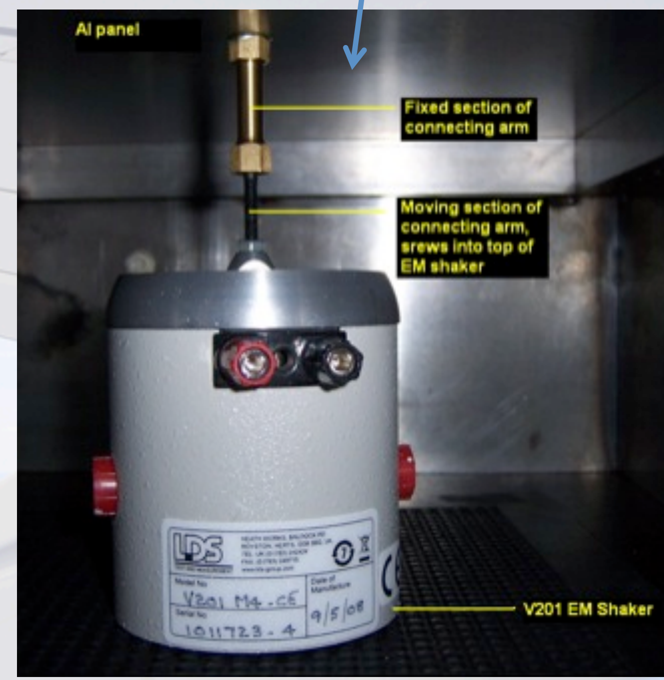

Base

amplitudes of +/- 0.1mm for wing panel subject to boundary layer turbulence

Harvester Positions

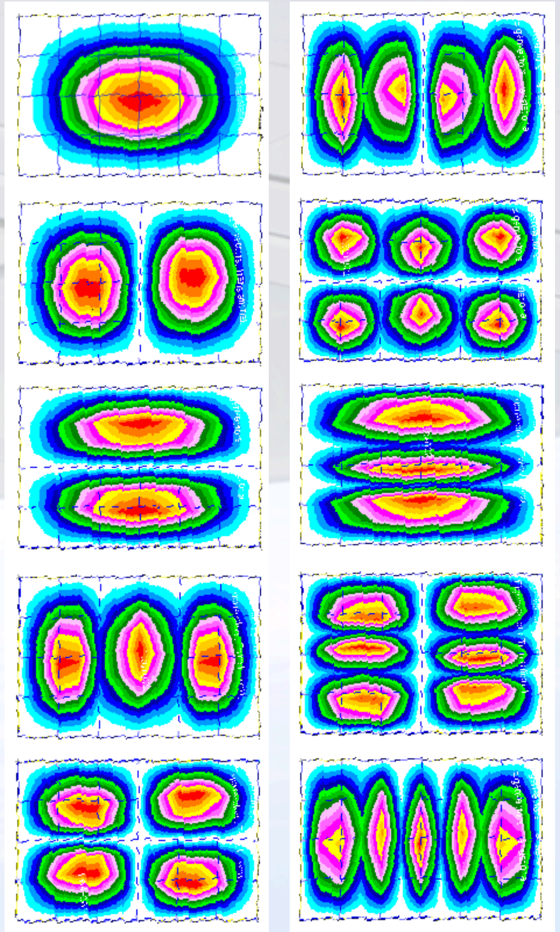

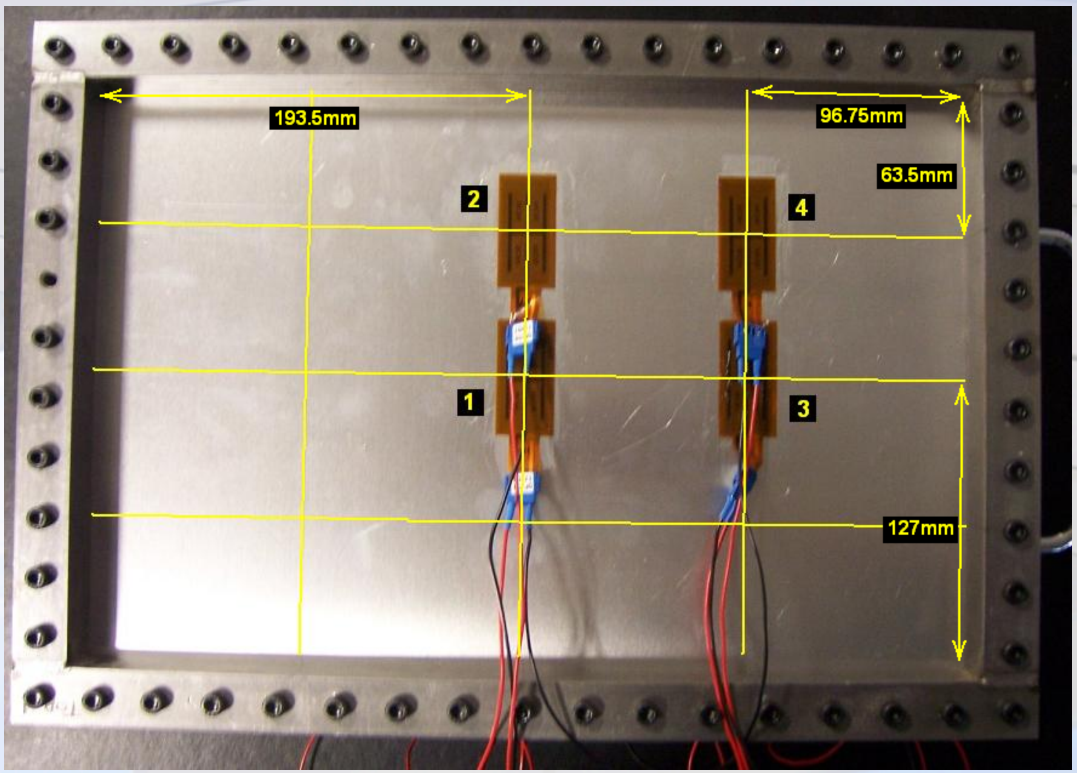

Initial Results

- Four harvester system

f, frequency (Hz)	Harvester number	V_{av}, mean voltage (V)	I_{av}, mean current (mA)	$Z_{real\,av}$, mean impedance, (kΩ)
40	1	1.86	0.0169	110
	2	0.95	0.0151	63
	3	0.71	0.0027	266
	4	0.71	0.0044	163
90	1	6.26	0.198	32
	2	0.96	0.0621	16
	3	0.84	0.0173	49
	4	0.91	0.0435	21
130	1	1.34	0.205	7
	2	1.22	0.117	10
	3	0.71	0.0242	29
	4	0.77	0.0782	10
200	1	17.5	1.34	13
	2	16.9	0.676	25
	3	5.28	0.0587	90
	4	5.34	0.206	26
300	1	15.2	1.25	12
	2	14.2	0.611	23
	3	4.01	0.196	21
	4	3.86	0.341	11

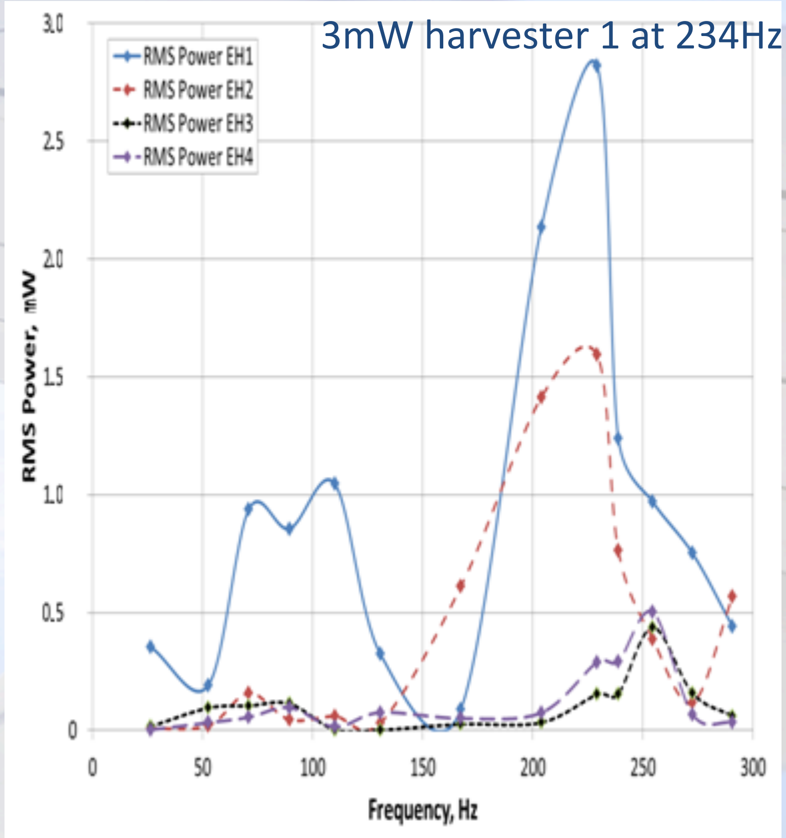

Harvester Positioning Optimisation Deflection of Built-in Plate

- For a plate with built-in edges deflection of the plate is described by:

$$w = \frac{w_0}{4}\left(1 - \cos\frac{2m\pi x}{a}\right)\left(1 - \cos\frac{2n\pi y}{b}\right)$$

- The bending strains experienced at the surface of the plate in the x-direction (ε_{Bx}) and y-direction, (ε_{By}) are

$$\varepsilon_{By} = \frac{t}{2}\frac{d^2w}{dy^2} \qquad \varepsilon_{Bx} = \frac{t}{2}\frac{d^2w}{dx^2}$$

- The membrane strains in the x and y directions is

$$\varepsilon_{Mx} = \frac{1}{2}\left(\frac{\partial w}{\partial x}\right)^2 \qquad \varepsilon_{My} = \frac{1}{2}\left(\frac{\partial w}{\partial y}\right)^2$$

Optimal position over a range of Frequencies

- Optimal position - maximum bending and membrane strains.
- Vibration frequencies /mode shapes vary throughout flight.
- Optimal position varies between vibration frequencies.
- Bending and strain equations over the entire frequency range:-

$$F(x,y) = \sum_{m} \sum_{n} \alpha_{mn} \frac{t}{2} w'' \omega_a \qquad F(x,y) = \sum_{m} \sum_{n} \alpha_{mn} \frac{1}{2} [w']^2 \omega_a$$

Cumulative Bending/Membrane Strain

Bending strains in x direction

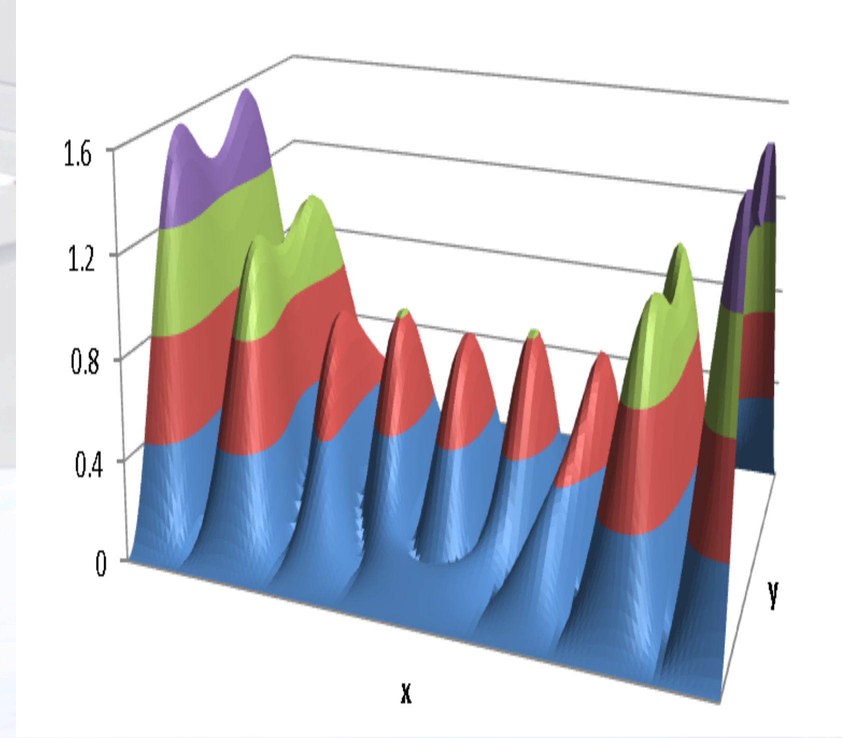

Membrane strains in x direction

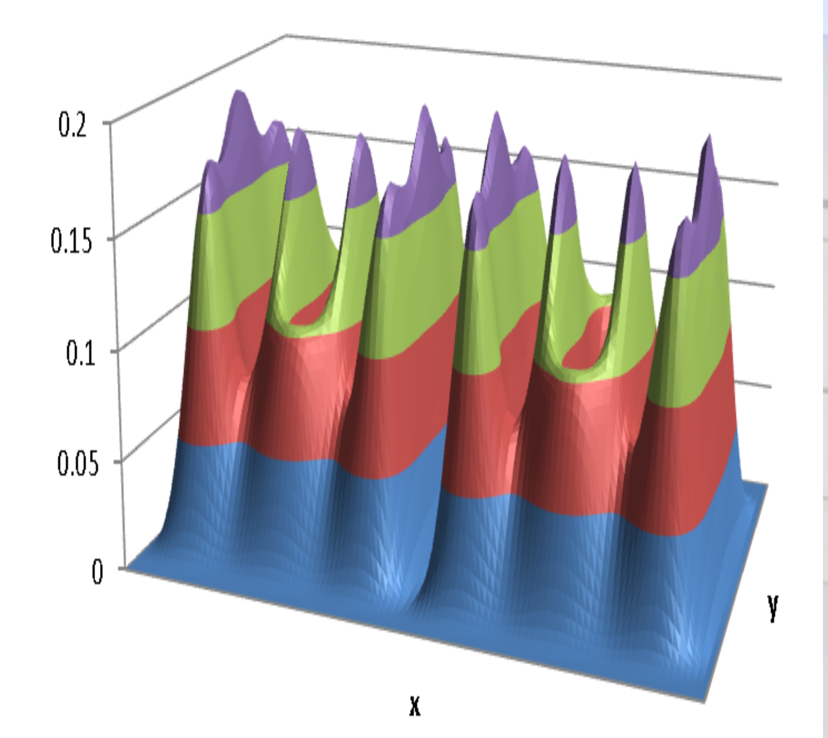

•Optimised using GA (NSGAII algorithm, population size: 100, simple multi point crossover: 0.95, simple be gene mutator: 0.05, number of generations: 100)

Optimal Position and Angle

- Strain at an angle calculated from components

$$\varepsilon_{max} = \pm\varepsilon_x cos\theta \pm \varepsilon_y sin\theta$$

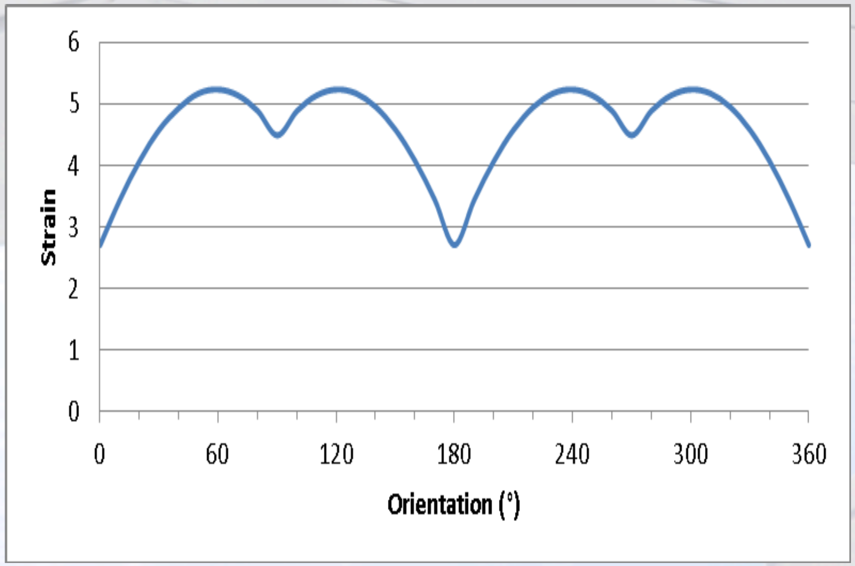

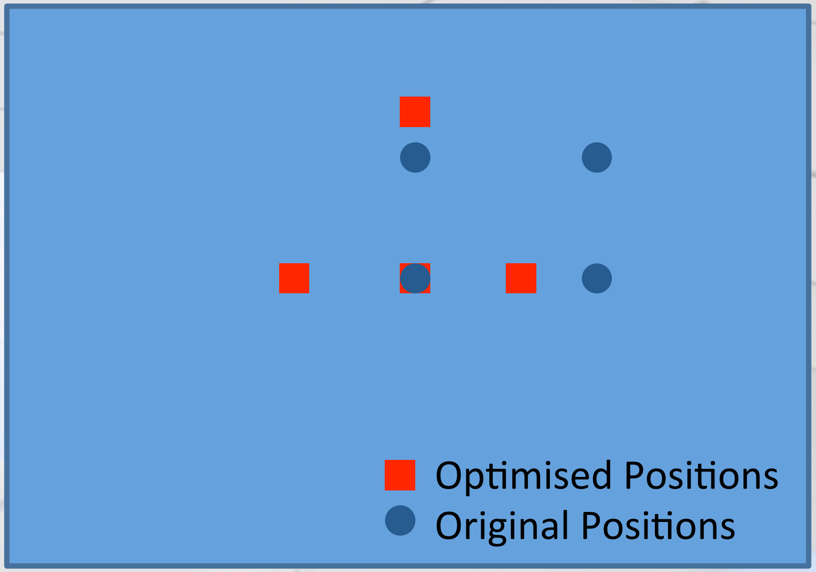

Experimental Validation

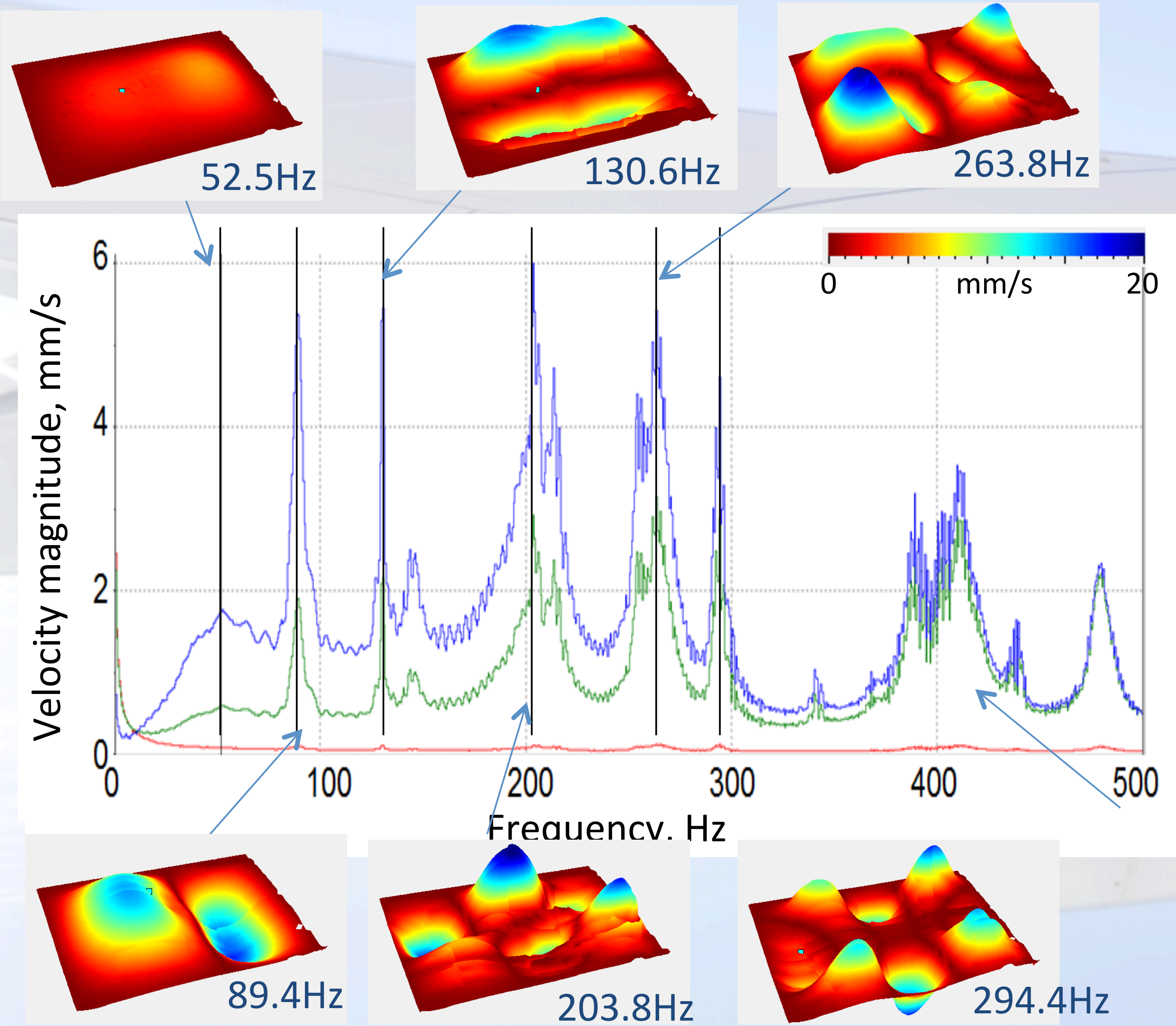

- 3D scanner laser vibrometer used
- To identify mode shapes
- To identify transition btwn mode shapes
- To measure amplitude

Active Vibration Harvesting

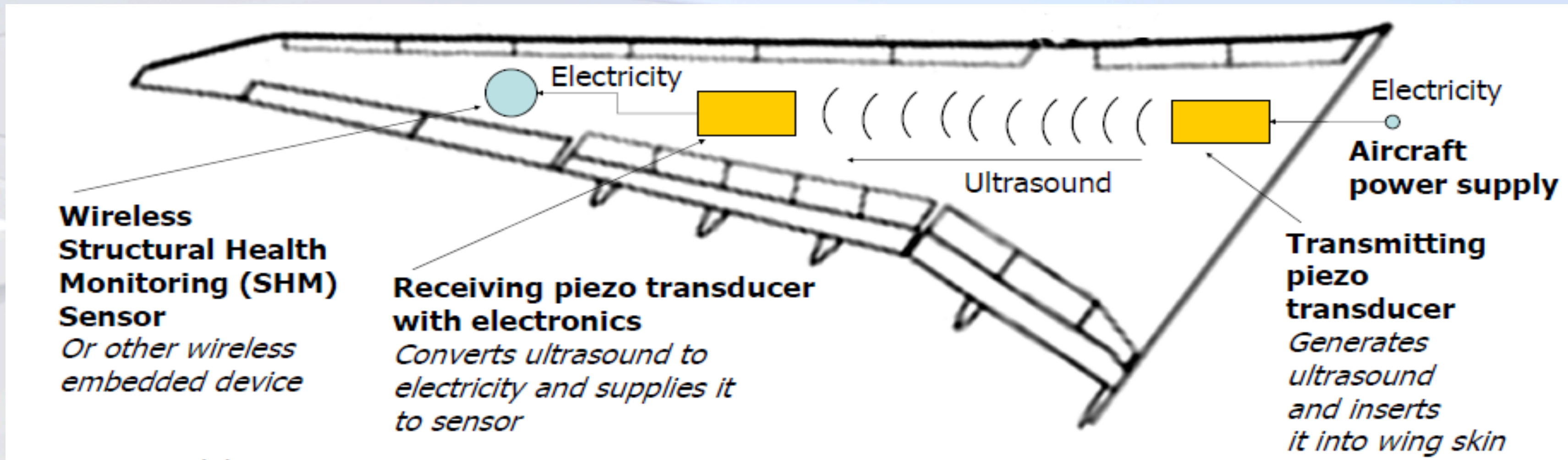

- Demonstrated using Quick Pack QP10n (Mide)

Prototype laboratory system:

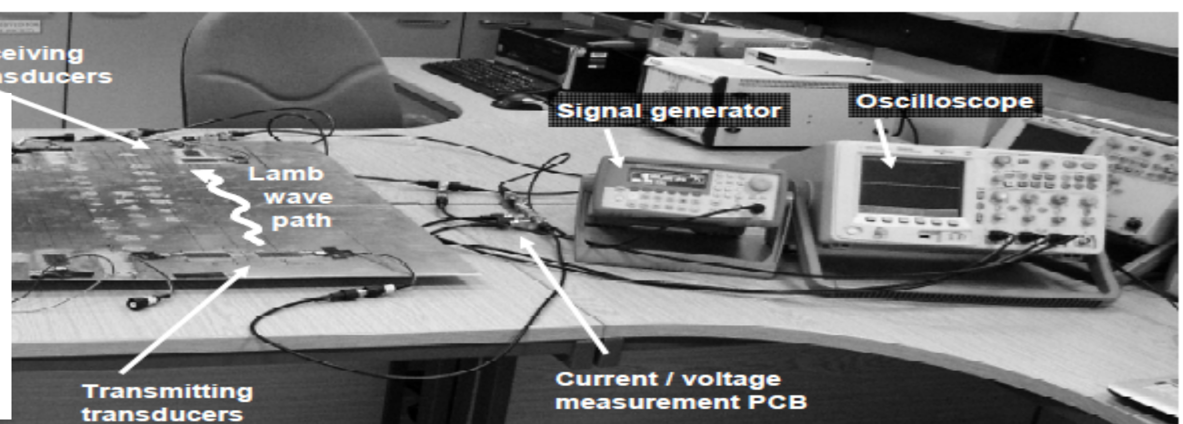

- McWade – crystal, narrow resonance, match transmit/ receive transducers.
- Quick Pack/MFC - thin sheet (solid/fibres), no resonant frequency, operate across range.

Active Vibration Harvesting

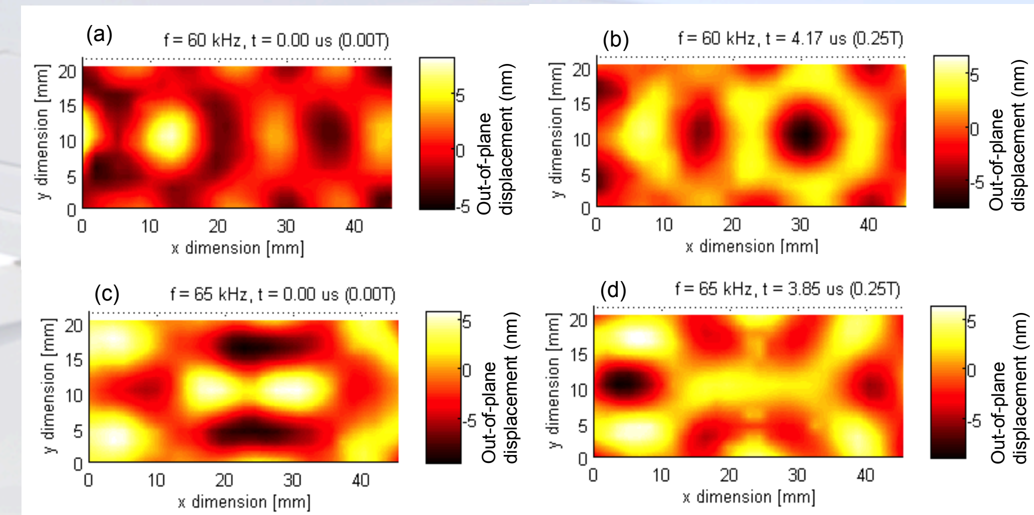

•Time domain maps of OOP vibration displacement at receiving transducer

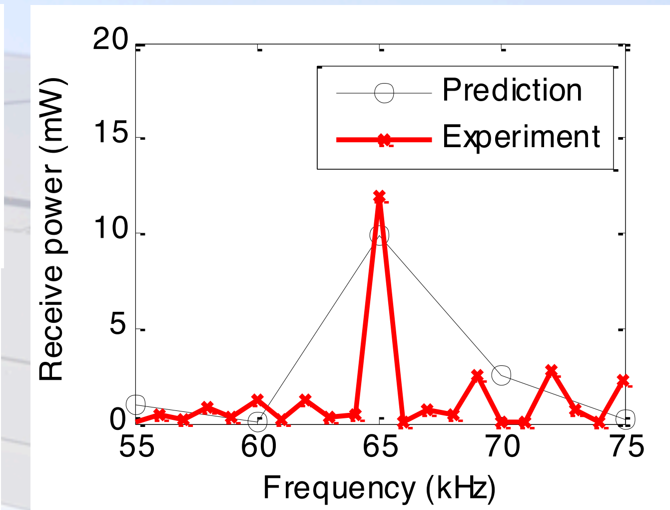

•Power delivered by the receiving transducer

- 17mW power transmitted across a distance of 540mm in 1.5mm thick aluminium plate driven by a signal of 20V amplitude at 224kHz f
- Power throughput can be easily increased by increasing the drive voltage

RF Energy Harvesting

RF Transmission

- Study CFRP/GFRP
- CFRP absorption increased rapidly with frequency
- GFRP almost transparent
- Focus two low frequency RF bands 13.56 MHz/ 125 kHz

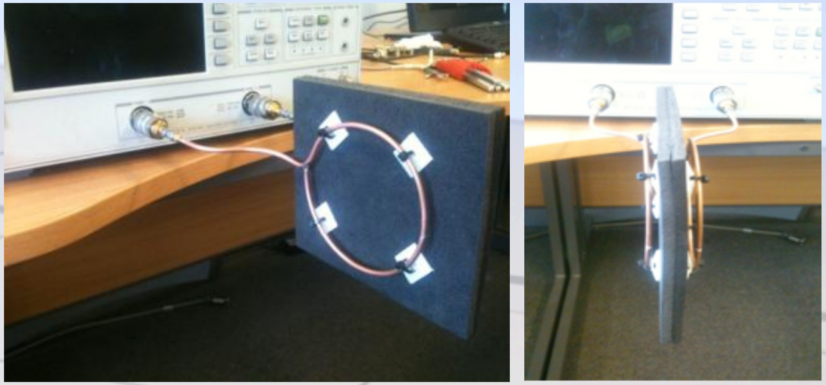

•The antenna used to measure transmission

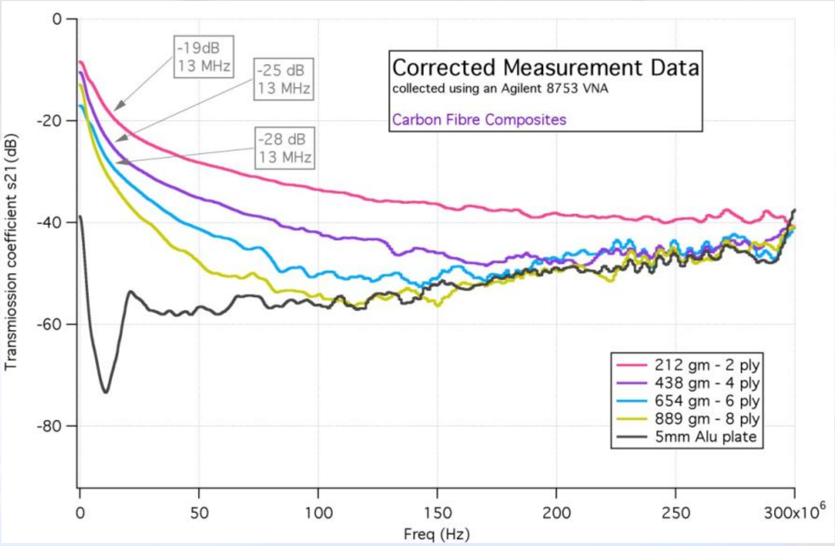

Power loss through CFRP

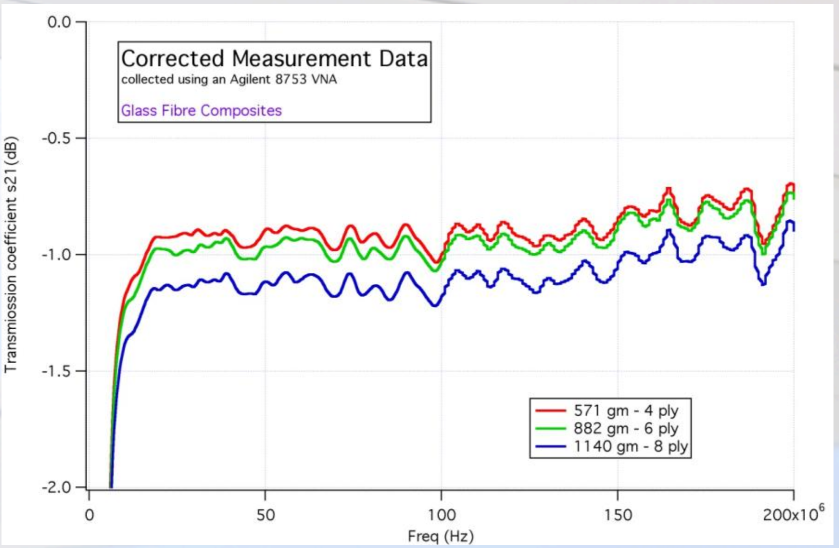

Power loss through GFRP

Power Management

Architecture of a Wireless Sensor Node Powered by TEG

- Hybrid storage

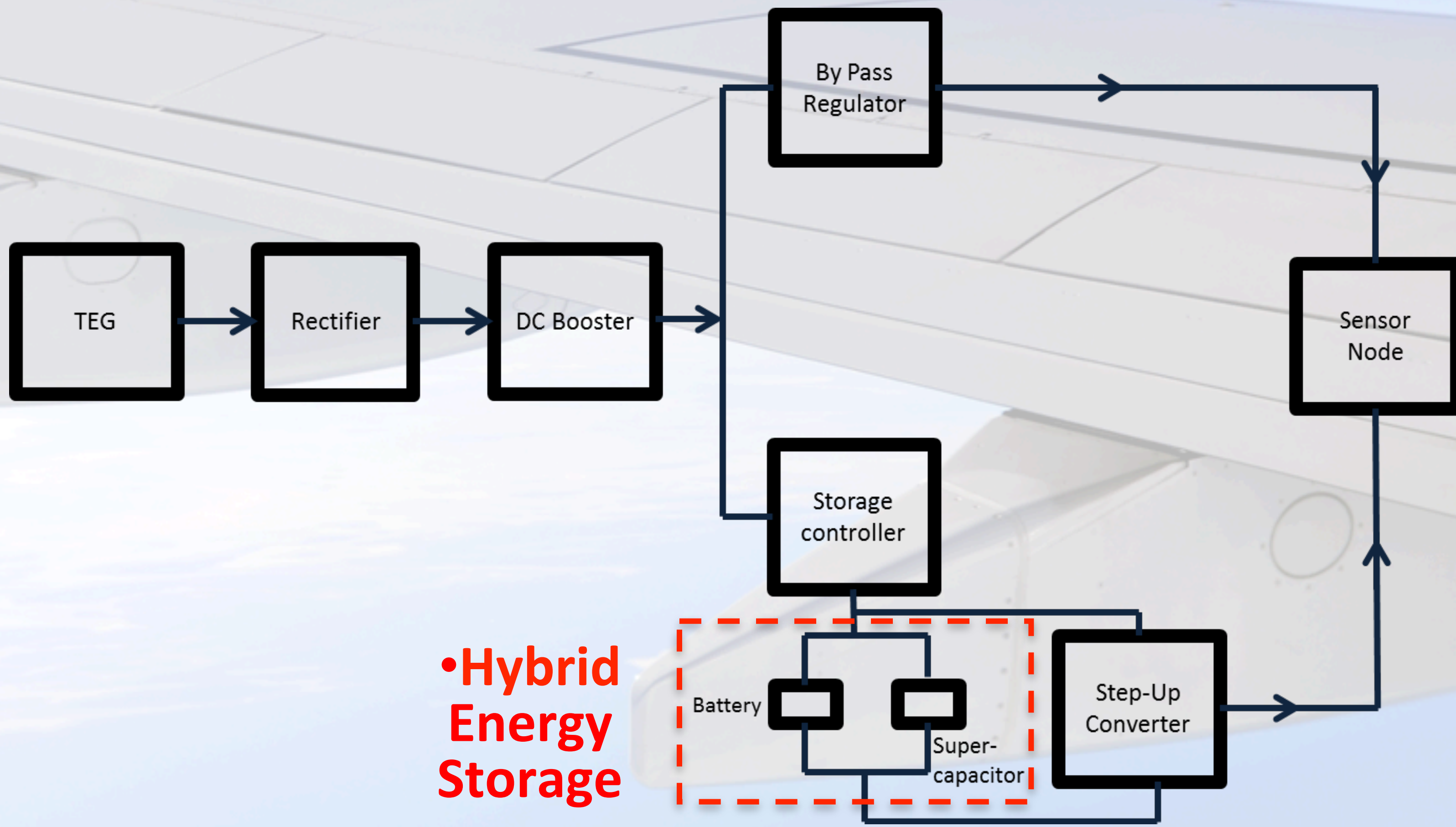

Energy Density vs Power Density

- The stored up energy should be from 40 J to 50 J
- Need to be able to operate between -40ºC to +85ºC
- Options include batteries and supercapacitors

- Sensor Node requires an energy storage unit that can
  - Store sufficient energy for prolonged, ‘normal’ operation
  - Be able to provide high current when required e.g. *wake-up* and *transmission* phases

Advantages of Hybrid Storage

- Can provide both energy and power density simultaneously
- The hybrid unit has a 3 J higher capacity than the Maxwell PC-10(5.54 F)
- The weight of hybrid system is almost half the weight of the supercapacitor

Storage Unit	Voltage Applied (V)	Energy (J)	Weight (g)
Maxwell PC-10 (2 in series: 5F)	4	41.32	12.6
MEC202+ Nesscap (Hybrid)	4	44.48	5.975

Advantages of Hybrid Storage

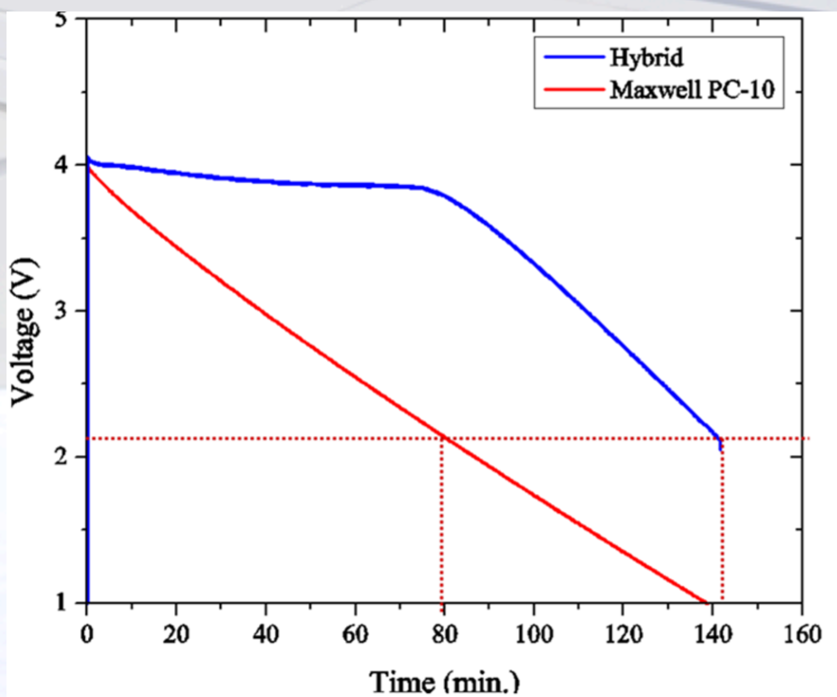

Discharge rate comparison of Maxwell and hybrid unit at +20°C

- Hybrid discharge 140 mins at +20°C, 120 mins in -20°C (due to temp dependent behaviour of battery (internal resistance increases at -ve temperature)
- Large voltage drops at battery eliminated by using supercapacitor in parallel giving a steady discharge (and hence extended runtime)
- The lower threshold voltage of battery also increased by parallel supercapacitor (also giving extended runtime)

Systems Integration

Systems Integration

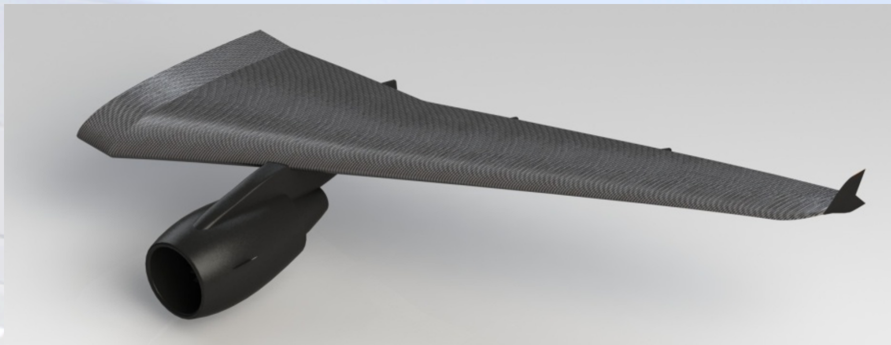

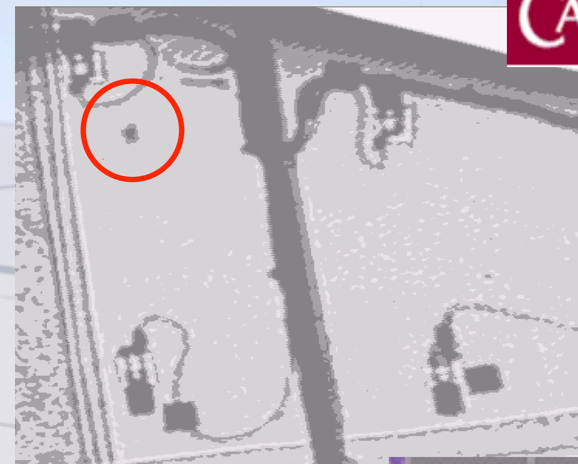

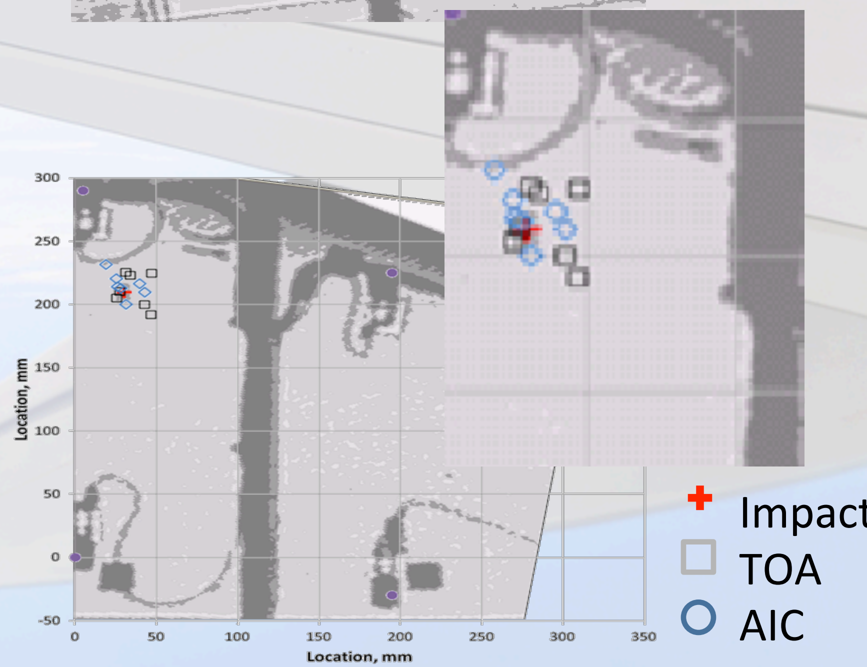

- Embedded multi-functional transducer for:
  - Acoustic Emission
  - Acousto-Ultrasonics
  - Vibration Energy Harvesting

Conclusions

- Considerable challenges in generating level of power required from energy harvesting and managing it efficiently
- Autonomous structural health monitoring device powered by energy harvesting is feasible
- Influence of sensing strategy